Cobalt magnetism in a superstructured metallic antiferromagnet $Na_{0.825}CoO_2$

Ben-Li Young,[1,*] P.-Y. Chu,[1] J. Y. Juang,[1] G. J. Shu,[2] and F. C. Chou[2,3]
[1]*Department of Electrophysics, National Chiao Tung University, Hsinchu City 30010, Taiwan*
[2]*Center for Condensed Matter Sciences, National Taiwan University, Taipei 10617, Taiwan*
[3]*National Synchrotron Radiation Research Center, Hsinchu City 30076, Taiwan*
(Received 31 May 2013; published 22 August 2013)

The Na atomic ordering and the local Co magnetism, in a metallic antiferromagnet made of $Na_{0.825}CoO_2$, are investigated by nuclear magnetic-resonance (NMR) techniques. Multiple well-resolved NMR peaks of ^{23}Na and ^{59}Co are observed, which suggests a superlattice structure forming in this Na-vacant cobaltate. Examining clues from published x-ray data, we refine the lattice superstructure so as to obtain the best description for the peaks seen in our NMR data. Magnetic Co ions are found to form a striped structure, which produces nontrivial magnetism. Analyzing the NMR frequency shift for each peak, we observe a frequency-shift anomaly, i.e., the breakdown of linearity between the NMR shift (that is, the local susceptibility) and the bulk susceptibility. We find that the shift anomaly can be described by an additional susceptibility component emerging at ∼60 K. Slow spin dynamics are observed near a metamagnetic transition where the spins flip between the antiferromagnetic and ferromagnetic orders. Unlike in ordinary spin glasses, this glassy behavior is induced by a magnetic field, which causes competition between the in-plane ferromagnetic and out-of-plane antiferromagnetic interactions, in a magnetic-frustrated triangular lattice.

DOI: 10.1103/PhysRevB.88.064418 PACS number(s): 76.60.−k, 75.47.Lx, 75.50.Ee

Sodium cobaltate, Na_xCoO_2, which was originally known as a battery material,[1] has been extensively studied for its other prominent features such as thermoelectricity,[2] superconductivity,[3] and magnetism.[4] The crystal consists of alternating layers of triangular Co lattice and Na. Varying the Na content changes the charge configuration (Co^{3+}, Co^{4+}) in the Co layers. Interestingly, the Na atoms form structural ordering patterns at certain sodium concentrations.[5] Due to the subtle interplay of the Na ordering with the charges and spins of the Co ions, a unique and rich phase diagram has been found.[6] Magnetic order occurs in the $x \geqslant 0.5$ region, but only at certain Na contents that produce a magnetic phase diagram displaying a discontinuous function of x. Recently, the phase diagram has been refined to the point at which only three distinct antiferromagnetic (AF) transitions were found.[7] Most notably, the $x \approx 0.82$ sample has the most stable AF phase and a well-defined superlattice structure. The local electronic properties and the Co magnetism, in connection with a resolved superstructure, have been investigated for $x = 1/2$ (a charge-ordered insulator),[8] $x = 2/3$ (a Curie-Weiss metal),[9] and $x = 1$ (a band insulator).[10] To obtain a more complete picture of this atypical magnetic phase diagram and superstructures, we conduct a nuclear magnetic-resonance (NMR) study on the antiferromagnetic phase of a Na_xCoO_2 single crystal with the stable concentration $x = 0.825$.

We find that both the ^{59}Co and ^{23}Na NMR spectra of $Na_{0.825}CoO_2$ show multiple well-resolved peaks. This confirms the existence of Na ordering in this crystal. By analyzing the NMR spectra, using clues from x-ray diffraction,[11] we derive a three-dimensional Na-stacking superstructure model that best describes our NMR spectra. Analyzing these peaks, we observe a NMR frequency-shift anomaly, that is, a breakdown in linearity between the peak frequency shift (i.e., the local susceptibility) and the bulk magnetic susceptibility. We discover that an additional local magnetic susceptibility component, emerging at ∼60 K, is the cause of the anomaly. We also observe a similar metamagnetic transition between the antiferromagnetic and ferromagnetic orders, as reported in $Na_{0.85}CoO_2$.[12] A time-dependent NMR spectrum, however, is observed near the metamagnetic transition. Unlike in ordinary spin glasses, this glasslike behavior is induced by a magnetic field and is caused by the competition between the in-plane ferromagnetic and out-of-plane antiferromagnetic interactions, in a magnetically-frustrated triangular lattice. Details of our experiments are described below.

For our NMR experiments, we use a single crystal of high-quality $Na_{0.825}CoO_2$. This sample was prepared and characterized by the same methods as described in Ref. 7. $Na_{0.825}CoO_2$ has a long-range A-type AF order,[4] with a Néel temperature of $T_N = 22$ K, as shown in Fig. 1, of the magnetic susceptibility. Standard Hahn-echo pulse sequences were employed throughout our ^{23}Na and ^{59}Co NMR experiments. Figure 2 shows the temperature-swept spectra for their central ($|-1/2\rangle \leftrightarrow |+1/2\rangle$) transitions, with a magnetic field of 88 kG applied parallel to the crystalline c axis. Multiple peaks are observed, which are separated at ∼60 K. There are a total of six well-resolved peaks of ^{23}Na, along with four peaks of ^{59}Co, for the central transition (Fig. 3). These sharp peaks suggest that Na vacancies are not randomly distributed in this crystal but form a particular pattern; otherwise, the spectra would have been broader. From the peak numbers, we find that there are six different crystallographic sites for the Na atoms, along with four such sites for the Co atoms, which are also confirmed by analyzing their quadrupolar satellite peaks and the spectra for the magnetic field perpendicular to the c axis. We are aware that a similar ^{23}Na spectrum was reported in Ref. 13, for $Na_{0.75}CoO_2$. However, in this other report, there are only three ^{59}Co peaks, even though their $x = 0.75$ sample has the same $T_N = 22$ K as our $x = 0.825$ sample. We suspect that the Na atomic order in $Na_{0.75}CoO_2$ may not be much different from that in $Na_{0.825}CoO_2$.

Vacancies in the Na layers produce two distinct crystallographic Na sites, called Na1 and Na2.[14] Na1 is located directly between the two cobalt atoms in its neighboring Co

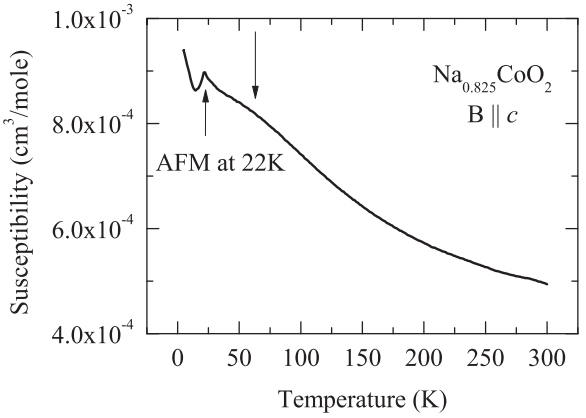

FIG. 1. Magnetic susceptibility of $Na_{0.825}CoO_2$, for a field applied along the crystalline c axis. Antiferromagnetic transition occurs at 22 K. The arrow at ~60 K denotes the deviation from Curie-Weiss behavior.

layers, whereas Na2 is sandwiched between the triangular Co sublattices. The two sites, Na1 in blue and Na2 in green, are illustrated in Fig. 4(a). By convention, the Co atoms, which

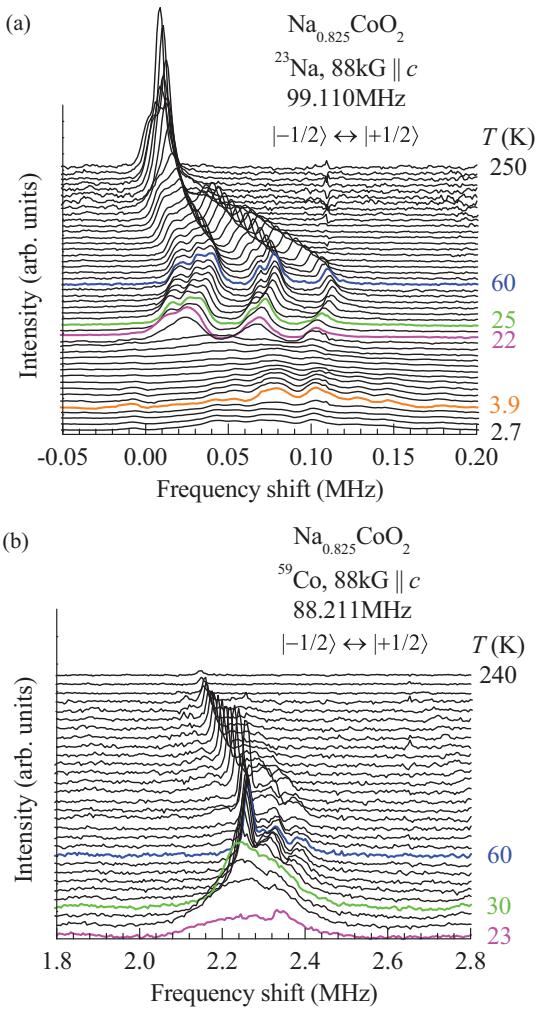

FIG. 2. (Color online) Temperature-swept (a) ^{23}Na and (b) ^{59}Co NMR spectra of $Na_{0.825}CoO_2$, for the $|-1/2\rangle \leftrightarrow |+1/2\rangle$ central transition, with a magnetic field applied along the crystalline c axis.

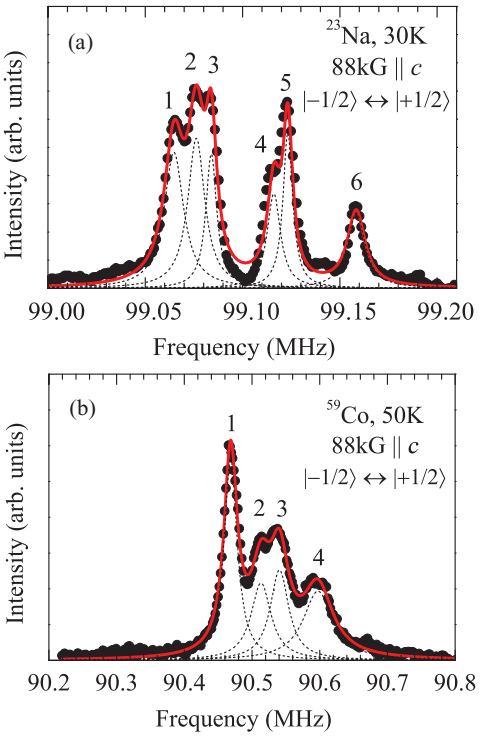

FIG. 3. (Color online) (a) ^{23}Na and (b) ^{59}Co NMR spectra of $Na_{0.825}CoO_2$, for a magnetic field applied along the crystalline c axis. In (a), there are six well-resolved peaks for the central transition ($|-1/2\rangle \leftrightarrow |+1/2\rangle$), while there are four peaks in (b).

are immediately above and below the Na1 atom, are called Co1, while the rest of the Co atoms are called Co2. Depending on the Na contents, Na vacancies can form different-sized clusters in Na_xCoO_2. Several models have been proposed experimentally and theoretically, but discrepancies exist.[5,15–18] For $Na_{0.825}CoO_2$, the trivacancy and quadrivacancy clusters are inferred from the vacancy clustering models proposed by Roger *et al.*[16] A divacancy cluster model with the superlattice unit-cell size $\sqrt{13}a \times \sqrt{13}a \times 3c$, however, was suggested based on x-ray-diffraction experiments.[7] With these pieces of information, we were motivated to examine all of the proposed vacancy cluster models, to search for the one that could reproduce the six Na and four Co sites obtained from our NMR experiments. However, none of them fit our NMR data. As is known, the $3c$ periodicity of the supercell along the c axis is confirmed according to Ref. 7, and this $3c$ periodicity is also seen in $Na_{2/3}CoO_2$.[9] Therefore, we repeated the search, keeping the $3c$ periodicity but tuning the supercell size a little bit. Eventually, we found that only Na divacancy clusters with a supercell size $\sqrt{12}a \times \sqrt{12}a \times 3c$ [Fig. 4(b)] gave the correct numbers of Na and Co sites seen in our NMR. This superlattice is formed by stacking the six $\sqrt{12}a \times \sqrt{12}a$ divacancy Na layers along the c axis, as illustrated in Fig. 4(b), where the Na vacancy layers are offset from each other by shifting a lattice vector [the arrows in Fig. 4(a)]. Six different Na sites and four Co sites are identified, as shown in Fig. 4(c), where the numbers next to the site labels denote the occupancies of these sites in a unit supercell. For this superstructure, the Na content is found to be $x = 0.833(= 10/12)$ which is very close to our nominal content of $x = 0.825$.

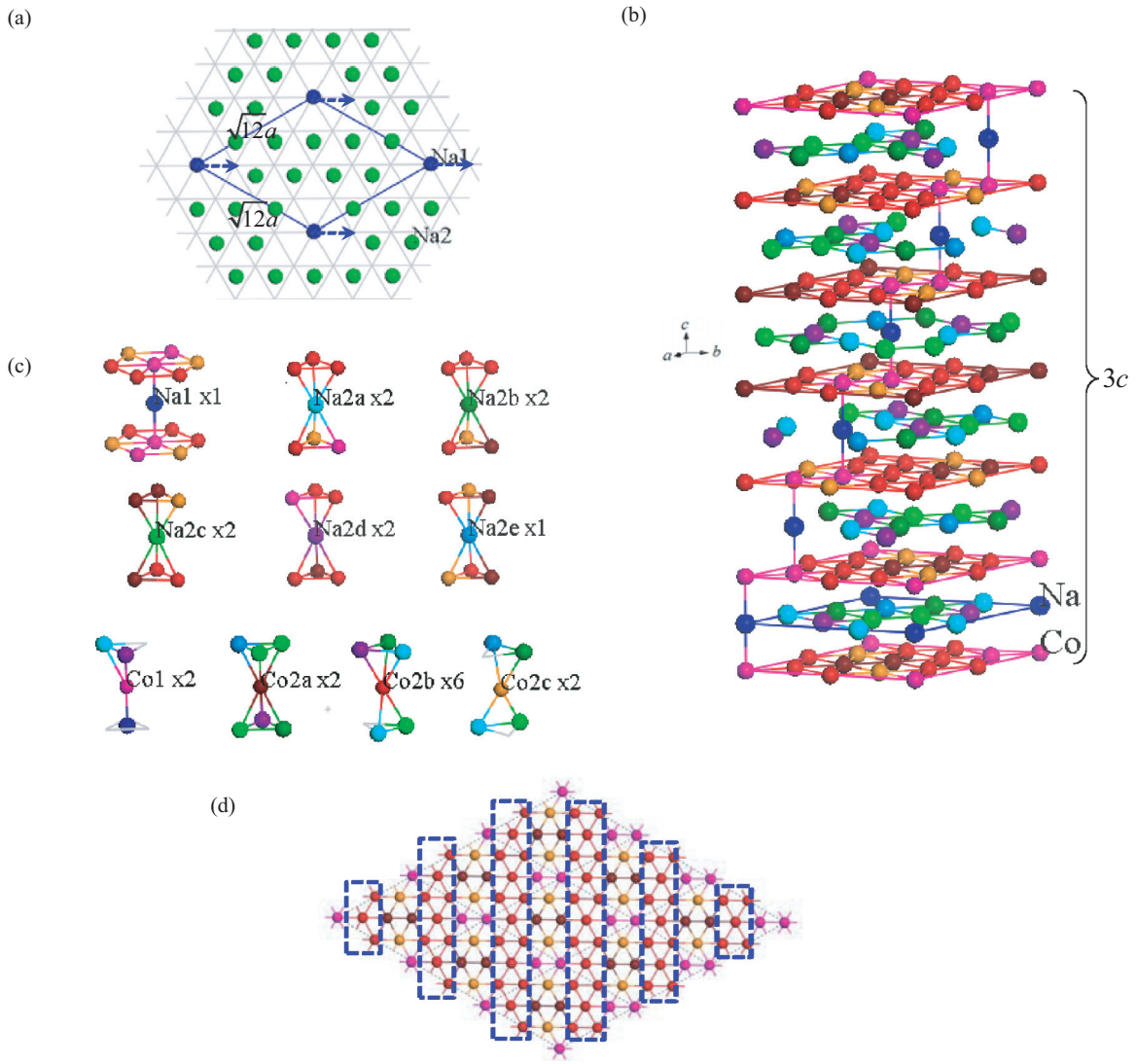

FIG. 4. (Color online) (a) A divacancy Na layer with the supercell size $\sqrt{12}a \times \sqrt{12}a$. (b) A three-dimensional superlattice model formed by stacking six of the divacancy Na layers which are offset from each other by shifting a lattice vector [the arrows in (a)]. The stacking period is $3c$ along the c axis. (c) The six different Na sites and four Co sites, extracted from (b). The numbers next to the site labels denote the occupancies of these sites in a unit supercell. (d) The Co2b sites forming a striped structure.

To further examine this superlattice model, we can compare the relative NMR peak intensity with the site occupancy for the different Na and Co sites. Note that a square of frequency correction and the spin-spin relaxation (T_2) effect must be taken into account, in order to obtain a true spectrum intensity.[9] We found that all six Na sites have a very similar T_2 relaxation time at 30 K, so that the Na peak intensities in Fig. 3(a) reflect the true site occupancy probability. We found that four of the peaks are of similar intensity; however, the fourth and sixth peaks have roughly half the intensity of the others. This is consistent with the relative site occupancies of Na, as shown in Fig. 4(c). The fourth and sixth peaks come from the Na1 and Na2e sites, while the other four peaks belong to the Na2a, Na2b, Na2c, and Na2d sites. At this moment, we do not have enough information to assign a specific peak to each Na site. As for the Co sites, we found that the T_2 effect is significant in calibrating the intensities in Fig. 3(b), where a peak at higher frequency has a faster relaxation rate of $1/T_2$, as seen in $Na_{2/3}CoO_2$.[9] The correct intensity ratio that we obtained for peaks 1 to 4 is 1 : 0.7 : 1 : 2.3. We consider this ratio to be compatible with the occupancy ratio 1 : 1 : 1 : 3 in Fig. 4(c), with the fourth peak assigned to the Co2b site. The poor accuracy in comparing intensities could be due to experimental error, since the NMR pulse parameters were optimized for the first Co peak only, and the same pulse parameters were used for obtaining the other Co peaks.

Figure 5 shows the ^{23}Na NMR spectrum for magnetic fields $B \perp c$ and $B \parallel c$. The quadrupolar satellites are barely seen in the $B \perp c$ spectrum, because they are scattered on both sides of the central peaks, unlike those in the $B \parallel c$ spectrum. The NMR resonance peak frequency for the transition $|m\rangle \leftrightarrow |m-1\rangle$ is determined by the equation $f = (\gamma/2\pi)[1 + K(\theta)]B + f_Q(m - 1/2)(3\cos^2\theta - 1 + \eta\sin^2\theta\cos 2\phi)/2$, where γ is the nuclear gyromagnetic ratio, K is the frequency shift, B is the applied magnetic field, f_Q is the nuclear quadrupolar frequency, and θ and ϕ are the polar and azimuthal angles

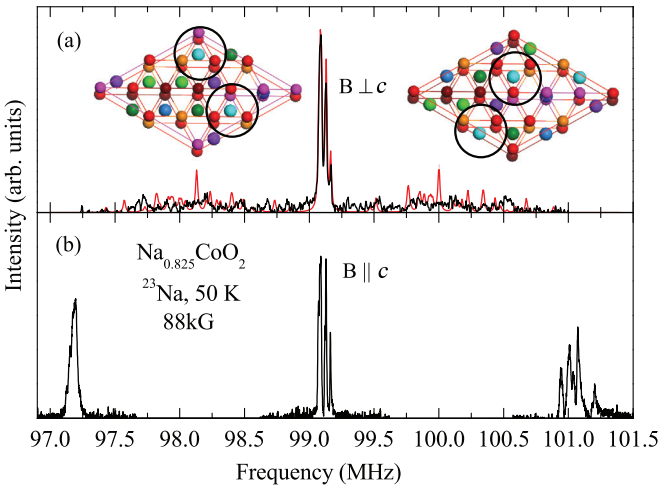

FIG. 5. (Color online) ^{23}Na NMR spectra of $Na_{0.825}CoO_2$ for magnetic fields applied (a) perpendicular and (b) parallel to the crystalline c axis. The red curve in (a) is a simulated spectrum. Two Na layers, extracted from the top two Na layers in Fig. 4(b), are illustrated here to show that the four Na2a (cyan) sites have a different azimuthal angle, ϕ, when $B \perp c$.

of the magnetic field relative to the principle axes of the electric-field gradient (EFG).[19] η is an asymmetry parameter that characterizes the axial symmetry of the EFGs. $\eta = 0$ when the nuclear site is uniaxially symmetric. According to Fig. 4(c), none of the Na sites possess uniaxial symmetry, so $\eta \neq 0$ for all of the Na sites, and their quadrupolar satellite peaks depend on ϕ when $B \perp c$. For a spectrum in this field direction, the angle ϕ is not the same for all Na2a sites in a unit supercell, because their EFG principle axes are oriented differently with respect to the magnetic field for such three-dimensional stacking of the Na layers, as illustrated in Fig. 5. Four different ϕ's are found for the Na2a site, as well as for the Na2b, Na2c, and Na2d sites; two ϕ's are found for the Na2e site, but only one ϕ is found for the Na1 sites. Since each ϕ gives a set of quadrupolar satellite peaks, a total maximum number of 19 $(=4 \times 4 + 2 + 1)$ quadrupolar peaks are expected to scatter on each side of the central peaks. A simulated spectrum is shown in Fig. 5(a), which qualitatively captures the features of the experimental curve. Due to many different Na sites in a supercell, there are too many degrees of freedom (such as η and ϕ) to fit the spectrum properly. We therefore simulated the spectrum by simply assigning certain values of η and ϕ for each of the Na sites. We did not try to manipulate these parameters to make the simulation look close to the experimental data. The simulation is just to illustrate the fact that, when B is applied perpendicularly to the c axis, there is indeed more than one ϕ angle for most of the Na sites, so that the quadrupolar peaks are scattered. This indirectly confirms the site symmetry. Overall, this proposed superlattice model, after numerous trials, is the only structure that we could find to adequately describe our NMR data and to give the Na content $x = 0.833$ close to our nominal $x = 0.825$.

Here we stress that the superstructure that we derived is not simply a coincidence, because it explains the NMR peak numbers, peak intensities, and the underlying site symmetry. Moreover, it reproduces the similar Na content as the nominal content. Only the supercell size ($\sqrt{12}a \times \sqrt{12}a$) is not consistent with that ($\sqrt{13}a \times \sqrt{13}a$) from the diffraction experiments. However, the two techniques should be complementary, not contradictory, in the structure determination. Note that the diffraction experiments were carried out at room temperature and zero magnetic field,[7] while our NMR were conducted at low temperature and 88 kG. The only possible reason that we can think of for the discrepancy is a rearrangement of the Na order at low temperature or under a magnetic field. Since the cooling rate was found to influence the Neel state in some of the samples showing 22-K Neel temperature,[20] we suspect that stress caused by thermal contraction, or possibly a magnetostrictive effect, might cause some minute difference in the Na ordering.

Recently Alloul *et al.* suggested that the pure-phase Na_xCoO_2, showing a 22-K Néel temperature, exists only for the $x = 10/13 \approx 0.77$ concentration,[20] which is different from our $x = 10/12 \approx 0.833$. There has been an ongoing debate on the exact Na content of this phase, as mentioned in their paper. While we are confident of our Na estimation, an argument on this issue is not the scope of this work. The superstructure that we derived is also notably different from theirs. They obtained a two-dimensional unit-cell size of $\sqrt{13}a \times \sqrt{13}a$ with Na trivacancies, while our unit cell is $\sqrt{12}a \times \sqrt{12}a$ with Na divacancies [Fig. 4(a)].

Interestingly, the magnetic Co2b sites in our model are arranged in a striped structure [Fig. 4(d)]. Cobalt atoms situated in such a superstructure could produce nontrivial electron correlation and collective magnetic behavior. We notice that the magnetic susceptibility curve in Fig. 1 deviates from the Curie-Weiss behavior at ~60 K, before entering the AFM phase. This is often attributed to the onset of short-range magnetic correlation or ordering.[4,12] However, we find that the ^{23}Na and ^{59}Co NMR spectra, at 60 K, do not show apparent line broadening, as expected for any short-range magnetic ordering. Their linewidths do not increase significantly until the temperature is close to 30 K, before entering the AFM transition at 22 K. The crystal electric-field effect is ruled out here, because the splitting between the lower-lying t_{2g} and higher-lying e_g bands is ~2.5 eV, which is much higher than 22 K.[21] Since the NMR frequency shift is a measure of the local magnetic susceptibility, we then compared the bulk susceptibility with the frequency shifts of all the Na and Co peaks, as shown in Figs. 6(a) and 6(b). Interestingly, the local susceptibility deviates from the bulk susceptibility, usually called a shift anomaly,[22] at the same temperature as that at which the Curie-Weiss behavior breaks down. A shift anomaly is often observed in heavy-fermion systems and is typically attributed to the Kondo coherence associated with the localized f electrons.[22,23] This mechanism does not apply here because $Na_{0.825}CoO_2$ is a hole-doped band insulator of $NaCoO_2$.[10]

Figures 6(c) and 6(d) are plots of the Na and Co shifts with respect to the shifts of the first Na and Co peaks, respectively. The linear relation between the individual shifts is interrupted at ~60 K and then is restored at ~30 K. This suggests that the shift anomaly is not simply the result of the difference between the local and bulk susceptibilities. An additional local susceptibility component might emerge so

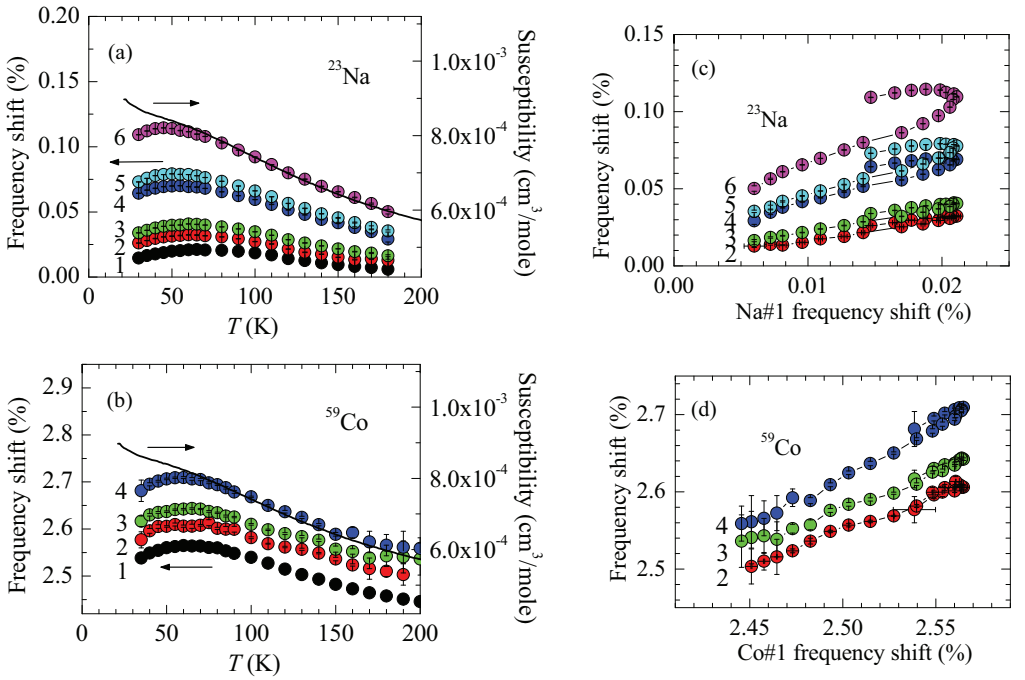

FIG. 6. (Color online) (a), (b) Comparisons of ^{23}Na and ^{59}Co NMR frequency shifts, respectively, with the bulk magnetic susceptibility. The curve labels denote the peak indices as assigned in Fig. 3. (c), (d) Plots of the ^{23}Na and ^{59}Co shifts vs the shifts of the first Na and Co peaks, respectively.

that the linearity of the frequency shifts between different nuclear sites is disrupted. We model the bulk susceptibility as $\chi(T) = [1 - f(T)]\chi_d(T) + f(T)\chi_0(T)$, where χ_d is the susceptibility from the localized d electrons and χ_0 is the emerging component.[22] The ratio of these two components is a function of temperature characterized by $f(T)$. The frequency shift then can be expressed as $K(T) = A_d\chi_d(T) + A_0\chi_0(T)$, where A_d and A_0 are the nuclear hyperfine coupling constants. This leads to a shift anomaly if $K(T)$ is rewritten as an explicit function of the bulk susceptibility $\chi(T)$. We can further express the shift of the jth Na (or Co) site, in terms of the shift of the ith Na (or Co) site, as $K_j(T) = (A_{d,j}/A_{d,i})K_i(T) + [A_{0,j} - (A_{d,j}/A_{d,i})A_{0,i}]\chi_0(T)$. This is linear if χ_0 is zero, and it deviates from linearity, once χ_0 appears. This expression could qualitatively explain what we saw in Figs. 6(c) and 6(d). According to this expression, $\chi_0(T)$ emerges at 60 K and then saturates so that the linearity recovers again. If the shift anomaly is caused by the short-range ordering, the breakdown of the linear relation in Figs. 6(c) and 6(d) should persist into the long-range order region. We do not know what specific correlation gives rise to $\chi_0(T)$ *a priori*, but this might not be unexpected, as the doped holes are distributed in a superstructured and mixed-valent Co^{3+}/Co^{4+} environment. In fact, a spin-orbital-polaron model was proposed to explain the magnetic susceptibility in $Na_{0.825}CoO_2$, where two spin liquids were suggested.[24] One spin liquid is from the localized $S = 1/2$ Co^{4+} ions, and the other is from the orbital polarons of the $S = 1$ Co^{3+} ions. The orbital polaron explains the large susceptibility at high temperatures, and the localized $S = 1/2$ Co^{4+} spin dominates the low-temperature Curie-Weiss susceptibility. According to Ref. 25, the orbital polaron

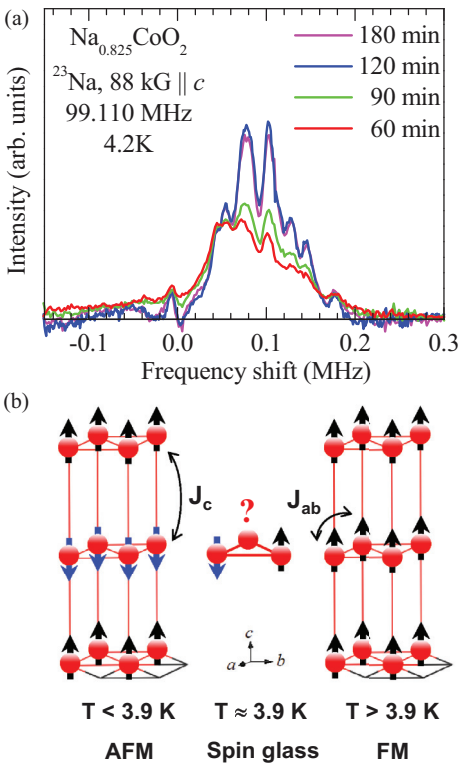

FIG. 7. (Color online) (a) Time-dependent ^{23}Na NMR spectra of $Na_{0.825}CoO_2$ at 88 kG and 4.2 K, near the AFM and FM phase boundary. (b) The magnetic structures of the AFM and FM phases in $Na_{0.825}CoO_2$. The Co spins in the triangular lattice are frustrated near the AFM-FM phase boundary (see text).

component diminishes at low temperature; however, this is contrary to the emergence in our observations.

$Na_{0.825}CoO_2$ has an *A*-type AFM order. When subjected to a magnetic field, it can undergo a metamagnetic transition, where the AFM state is spin flipped into a ferromagnetic (FM) state.[12] Our NMR spectra were taken at 88 kG, which happens to put the sample into a state near the metamagnetic phase boundary. According to Fig. 2, the sample first enters a FM state at 22 K and returns to an AFM phase at 3.9 K. At 4.2 K, we accidentally observed that the ^{23}Na spectrum showed time dependence after the sample was warmed up from 2.7 to 4.2 K. It took about 120 min for the sample to recover from the AFM state to FM state. This slow spin dynamics indicates that a spin glass might occur near the metamagnetic boundary. According to Ref. 26, the interlayer AFM exchange coupling is not much different from the intralayer FM exchange coupling, so a slightly inhomogeneous magnetic field in the sample might cause a mixture of the two phases. The spin frustration, due to the competing AFM and FM interactions, then could occur for the Co spins in a triangular lattice, as illustrated in Fig. 7(b). In principle, the conditions required for a spin glass, such as lattice disorder and spin frustration, are fulfilled in $Na_{0.825}CoO_2$. It would be interesting to further investigate this magnetic-field-induced glassy behavior, to see if it has properties similar to ordinary spin glasses.

In summary, we use NMR techniques to refine the three-dimensional superstructure for a single crystal of $Na_{0.825}CoO_2$, where a magnetic striped structure forms in the Co layers. An additional susceptibility component is found to emerge at $T \sim 60$ K. A magnetic-field-induced glassy behavior is observed near a FM-AFM metamagnetic phase boundary. The resolved superlattice model may shed light on the nature of the electron correlation and magnetic couplings in a frustrated mixed-valent environment that produces the metallic antiferromagnetism in $Na_{0.825}CoO_2$.

We thank M.-W. Chu for valuable discussions. This work is supported by National Science Council Grants No. 98-2112-M-009-016-MY3 and No. 101-2112-M-009-015-MY2 and by the MOE ATU Program operated at National Chiao Tung University.

*Corresponding author: blyoung@mail.nctu.edu.tw

[1] L. W. Shacklette, T. R. Jow, and L. Townsend, J. Electrochem. Soc. **135**, 2669 (1988).
[2] I. Terasaki, Y. Sasago, and K. Uchinokura, Phys. Rev. B **56**, R12685 (1997).
[3] K. Takada, H. Sakurai, E. Takayama-Muromachi, F. Izumi, R. A. Dilanian, and T. Sasaki, Nature (London) **422**, 53 (2003).
[4] S. P. Bayrakci, C. Bernhard, D. P. Chen, B. Keimer, R. K. Kremer, P. Lemmens, C. T. Lin, C. Niedermayer, and J. Strempfer, Phys. Rev. B **69**, 100410 (2004).
[5] H. W. Zandbergen, M. L. Foo, Q. Xu, V. Kumar, and R. J. Cava, Phys. Rev. B **70**, 024101 (2004).
[6] M. L. Foo, Y. Wang, S. Watauchi, H. W. Zandbergen, T. He, R. J. Cava, and N. P. Ong, Phys. Rev. Lett. **92**, 247001 (2004).
[7] G. J. Shu, F.-T. Huang, M.-W. Chu, J.-Y. Lin, P. A. Lee, and F. C. Chou, Phys. Rev. B **80**, 014117 (2009).
[8] J. Bobroff, G. Lang, H. Alloul, N. Blanchard, and G. Collin, Phys. Rev. Lett. **96**, 107201 (2006).
[9] T. A. Platova, I. R. Mukhamedshin, H. Alloul, A. V. Dooglav, and G. Collin, Phys. Rev. B **80**, 224106 (2009).
[10] G. Lang, J. Bobroff, H. Alloul, P. Mendels, N. Blanchard, and G. Collin, Phys. Rev. B **72**, 094404 (2005).
[11] F. C. Chou, M. W. Chu, G. J. Shu, F.-T. Huang, W. W. Pai, H. S. Sheu, and P. A. Lee, Phys. Rev. Lett. **101**, 127404 (2008).
[12] J. L. Luo, N. L. Wang, G. T. Liu, D. Wu, X. N. Jing, F. Hu, and T. Xiang, Phys. Rev. Lett. **93**, 187203 (2004).
[13] M.-H. Julien, C. de Vaulx, H. Mayaffre, C. Berthier, M. Horvatić, V. Simonet, J. Wooldridge, G. Balakrishnan, M. R. Lees, D. P. Chen, C. T. Lin, and P. Lejay, Phys. Rev. Lett. **100**, 096405 (2008).
[14] Q. Huang, M. L. Foo, R. A. Pascal, J. W. Lynn, B. H. Toby, T. He, H. W. Zandbergen, and R. J. Cava, Phys. Rev. B **70**, 184110 (2004).
[15] P. Zhang, R. B. Capaz, M. L. Cohen, and S. G. Louie, Phys. Rev. B **71**, 153102 (2005).
[16] M. Roger, D. J. P. Morris, D. A. Tennant, M. J. Gutmann, J. P. Goff, J.-U. Hoffmann, R. Feyerherm, E. Dudzik, D. Prabhakaran, A. T. Boothroyd, N. Shannon, B. Lake, and P. P. Deen, Nature (London) **445**, 631 (2007).
[17] Y. Hinuma, Y. S. Meng, and G. Ceder, Phys. Rev. B **77**, 224111 (2008).
[18] Y. S. Meng, Y. Hinuma, and G. Ceder, J. Chem. Phys. **128**, 104708 (2008).
[19] A. Abragam, *The Principles of Nuclear Magnetism* (Oxford University Press, Oxford, 1996).
[20] H. Alloul, I. R. Mukhamedshin, A. V. Dooglav, Y. V. Dmitriev, V.-C. Ciomaga, L. Pinsard-Gaudart, and G. Collin, Phys. Rev. B **85**, 134433 (2012).
[21] D. J. Singh, Phys. Rev. B **61**, 13397 (2000).
[22] N. J. Curro, B.-L. Young, J. Schmalian, and D. Pines, Phys. Rev. B **70**, 235117 (2004).
[23] E. Kim, M. Makivic, and D. L. Cox, Phys. Rev. Lett. **75**, 2015 (1995).
[24] M. Daghofer, P. Horsch, and G. Khaliullin, Phys. Rev. Lett. **96**, 216404 (2006).
[25] M. Daghofer, P. Horsch, and G. Khaliullin, in *Quantum Magnetism*, edited by B. Barbara, Y. Imry, G. Sawatzky, and P. Stamp, NATO Science for Peace and Security Series (Springer, New York, 2008), pp. 49–55.
[26] S. P. Bayrakci, I. Mirebeau, P. Bourges, Y. Sidis, M. Enderle, J. Mesot, D. P. Chen, C. T. Lin, and B. Keimer, Phys. Rev. Lett. **94**, 157205 (2005).